How Rapidly Does the SH Radical React with N_2O?

Scott C. Herndon,† Karl D. Froyd,† Edward R. Lovejoy, and A. R. Ravishankara*,†

National Oceanic and Atmospheric Administration, Aeronomy Laboratory, Boulder, Colorado 80303-3328

Received: April 8, 1999; In Final Form: June 23, 1999

The reaction of SH radical with N_2O was investigated by using two complementary experimental methods: (a) a pulsed photolysis apparatus where SH was detected via laser-induced fluorescence and (b) a discharge flow tube where SH was detected via chemical ionization mass spectrometry. The rate coefficient for this reaction, k_1, was found to be less than 5×10^{-16} cm^3 molecule^{-1} s^{-1} at 298 K, in contrast to the large value reported in the literature [Ravichandran; et al. *Chem. Phys. Lett.* **1994**, *217*, 375−379]. Secondary reactions were deduced to be unimportant in our system. Some possible reasons for the previously reported high value are presented. The low value of k_1 makes the oxidation of SH by N_2O and removal of N_2O by SH unimportant in the earth's atmosphere.

Introduction

Hydrogen sulfide (H_2S), a predominantly terrestrial emission, is one of the important natural sources of atmospheric sulfur.[1] In the troposphere, H_2S is removed mostly via its reaction with the OH radical, which produces the SH radical.[2] The reactions of SH with O_3 and NO_2 ($k(298) = 3.5 \times 10^{-12}$ and 6.5×10^{-11} cm^3 molecule^{-1} s^{-1}, respectively[3]) are the main pathways for removal of SH and give it an atmospheric lifetime of less than a second. Oxidation of SH eventually leads to SO_2.

It has been reported[4] that SH reacts rapidly with N_2O, a gas that is believed to be unreactive in the troposphere,[5] to form HSO.

$$SH + N_2O(0, 0, 0) \rightarrow HSO + N_2; \quad k_1,\ \Delta^\circ H_{rxn}(298K) \approx -55 \text{ kcal mol}^{-1} \quad (1)$$

In the above reaction, (0, 0, 0) denotes the vibrational ground state of N_2O. The enthalpy of reaction 1 was calculated from tabulated data.[3] Ravichandran et al.[4] report a value of k_1 at 298 K of $(1.3 \pm 0.14) \times 10^{-11}$ cm^3 molecule^{-1} s^{-1}. They photolyzed H_2S at 193 nm to produce the SH radical, in varying pressures of N_2O, and measured the temporal profiles of the resulting HSO chemiluminescence to deduce k_1. If reaction 1 is as rapid as they report, the mechanism of H_2S oxidation and lifetime of N_2O in the atmosphere will have to be revised significantly. A rough estimate[6] of the average SH radical concentration in the lower troposphere is 1×10^2 molecules cm^{-3}. Even such a low concentration of SH would lead to an atmospheric lifetime of roughly 24 years for N_2O with respect to reaction 1 if the value reported by Ravichandran et al. is used. A lifetime of 24 years for N_2O is 5 times smaller than the currently accepted value of around 120 years.[5] Even if SH is isolated to a few regions (i.e., terrestrial boundary layer), it would still significantly reduce the currently accepted N_2O lifetime if the reported value of k_1 were correct. A short lifetime of N_2O (due primarily to seasonal H_2S emissions) is inconsistent with the observed invariability of its abundance[5] with season and location, and other sources of N_2O would be required to balance its atmospheric budget.

The title reaction is also interesting because the analogous reaction, $OH + N_2O \rightarrow HO_2 + N_2$, is also exothermic ($\Delta^\circ H_{rxn} \approx -9$ kcal mol^{-1}) but very slow,[7] $\sim 3.8 \times 10^{-17}$ cm^3 molecule^{-1} s^{-1}. (Continuing work in our laboratory places an upper limit for this rate constant at less than 8×10^{-18} cm^3 molecule^{-1} s^{-1}.) This low value is to be contrasted with the reported high value of k_1.

This paper reports an upper limit of k_1 determined using two experimental methods: pulsed photolysis laser-induced fluorescence (PP-LIF) and discharge flow chemical ionization mass spectrometry (DF-CIMS). We find k_1 is less than 5×10^{-16} cm^3 molecule^{-1} s^{-1}, which sharply contrasts with the report of Ravichandran et al.[4] The possibility that secondary reactions are responsible for the measured low value of k_1 is also discussed and shown to be very unlikely.

Experiments and Results

The initial experiments were carried out using pulsed laser photolysis of H_2S as a source of SH. Because we obtained values of k_1 that were significantly lower than that reported in the literature, we also measured k_1 using a different experimental system that avoids photolysis and the consequent secondary reactions. For ease of presentation, these two experiments and their results are discussed below in separate sections.

PP-LIF. The apparatus and procedures used for studying the reactions of SH are very similar to those used to measure the rate coefficients for reactions of the OH radical[8] and the CH_3S radical.[9] Therefore, only the description of the SH detection and a few details necessary to understand this work are given here. Figure 1 shows the schematic of the pulsed photolysis laser-induced fluorescence apparatus. The SH radical was generated by pulsed laser photolysis of H_2S, and its temporal profile was measured by pulsed laser-induced fluorescence.

$$H_2S \xrightarrow{h\nu/193\text{ nm}} H + SH \quad (2)$$

* To whom correspondence should be addressed. NOAA/ERL, R/E/AL2, 325 Broadway, Boulder, CO 80303. E-mail: ravi@al.noaa.gov.

† Also affiliated with Department of Chemistry and Biochemistry, University of Colorado, Boulder, Colorado, and The Cooperative Institute for Research in Environmental Sciences, University of Colorado, Boulder, Colorado.

10.1021/jp9911853 CCC: $18.00
Published on Web 08/06/1999

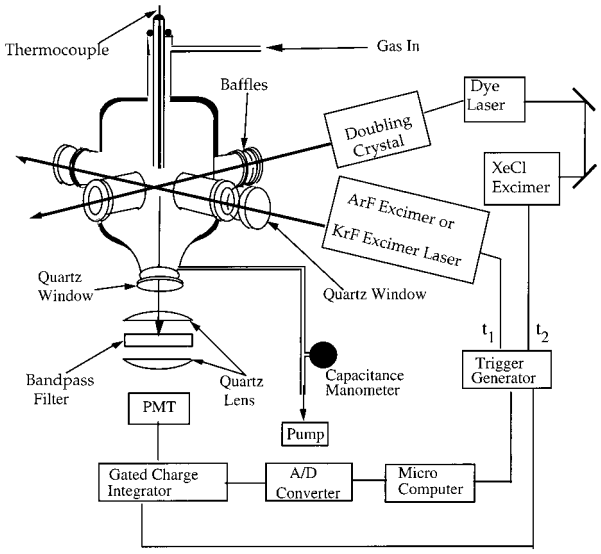

Figure 1. Schematic of the pulsed photolysis apparatus used to study reactions of SH radicals. SH radicals were generated by pulsed laser photolysis of H_2S and were detected by pulsed laser-induced fluorescence. The components of the apparatus are marked in the figure.

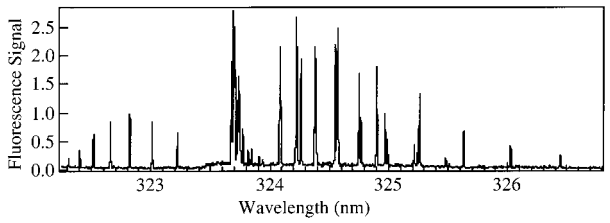

Figure 2. Fluorescence excitation spectrum of SH measured in this study. SH was generated by pulsed photolysis of H_2S at 193 nm. This spectrum was acquired using a 355 ± 12 nm band-pass filter, delay time of 100 μs, $[H_2S] \approx 3 \times 10^{14}$ molecules cm^{-3}, 80 Torr of N_2 total pressure, and a photolysis energy of 5 mJ pulse^{-1}. The line shapes and peak positions of this excitation spectrum did not change in the presence of 12 Torr of N_2O. The "bump" beginning near 323.6 nm and tailing off with longer wavelength is not due to SH but, as will be discussed in a forthcoming paper, is likely an LIF signal due to SO.

All rate coefficients were measured at 295 ± 3 K in 30−120 Torr of N_2 (or 100 Torr of He).

Laser-induced fluorescence of SH ($A^2\Sigma \leftarrow X^2\Pi$) was excited by the output of an excimer-pumped dye laser. A photomultiplier tube (PMT) was placed at right angles to the photolysis and the excitation laser beams. A band-pass filter was placed between the PMT and the reaction zone to allow maximal transmission at 355 ± 12 nm and thus detection of fluorescence from the ($0 \rightarrow 1$) vibronic manifold. This filter discriminated against scattered light from the photolysis and probe lasers. Figure 2 shows an excitation spectrum of SH taken 100 μs after its production via the 193 nm photolysis of H_2S in 80 Torr of N_2 total. This spectrum is in excellent agreement with other published excitation spectra.[10,11] The line shape and peak locations were unchanged in the presence of 12 Torr of N_2O. The probe laser frequency was scanned to locate the fluorescence peak corresponding to the $^RQ_{21}$ ($\lambda \approx 323$ nm) transition in the $^2\Sigma \leftarrow {}^2\Pi$ manifold. Excitation at this peak was used to monitor SH in kinetics experiments described below.

The sensitivity for SH detection was calculated to be $\sim 8 \times 10^8$ molecules cm^{-3} (averaging 100 laser shots) by measuring the LIF signal from a known concentration of SH. The concentration of SH was calculated using measured concentrations of H_2S and photolysis fluence. The fluence was measured using a calibrated thermopile detector. The detection limit is defined as a signal-to-noise ratio of 1, where the noise is twice the standard deviation of the mean of the PMT signal measured in the absence of SH (i.e., background) and the signal is the value above this background. The initial concentration of SH almost never exceeded 8×10^{10} molecules cm^{-3} (the exception is noted later).

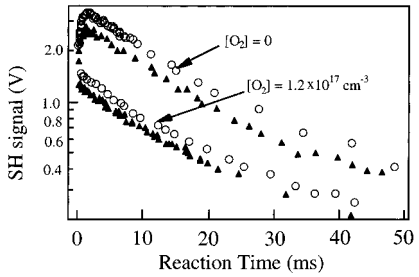

Figure 3. Temporal profiles of SH measured in the absence (open circles) and the presence (triangles) of $>1 \times 10^{17}$ molecules cm^{-3} N_2O in the PP-LIF system. The upper profiles were measured in the absence of O_2. The increase in SH signal at short times is due to the reaction of H atoms with H_2S. The lower profiles were measured in the presence of O_2 (3.7 Torr), which scavenged H atoms and suppressed the secondary production of SH. The time constant for the decay of SH was the same within the precision of the data in all cases. The initial SH concentrations were $(4-7) \times 10^{10}$ molecules cm^{-3}. The total system pressure was 93−107 Torr. The signal levels are consistent with the recorded precursor concentrations and photolysis fluences.

The concentrations of N_2, He, O_2, a 2% H_2S mixture with He, and N_2O in the reaction cell were calculated from their flow rates measured using calibrated electronic mass flow meters. Pressure and temperature were measured using a calibrated capacitance manometer and a thermocouple probe, respectively. Both UHP (>99.99995%) He and N_2 (>99.9995%) were used as carrier gases.

Some typical SH temporal profiles acquired in the PP-LIF experiments are shown in Figure 3. H_2S photolysis at 193 nm yields SH and H atoms. H atoms react with H_2S to generate more SH on a time scale that depends on the concentration of H_2S.

$$H + H_2S \rightarrow H_2 + SH \qquad (3)$$

The rate coefficient for reaction 3 at 298 K has been measured[12,13] to be $\sim 7 \times 10^{-13}$ cm^3 molecule^{-1} s^{-1}. Thus, the temporal profiles of SH should have a rise due to reaction 3 and a decay due to SH loss. Such biexponential temporal profiles were indeed observed (Figure 3). Addition of O_2 scavenged the H atoms to make HO_2,

$$H + O_2 \xrightarrow{M} HO_2 \qquad (4)$$

and suppressed the secondary production of SH. Therefore, a single-exponential decay of SH was observed when sufficient O_2 was present to scavenge H atoms (Figure 3). The rate coefficient for the reaction of HO_2 with H_2S is less than 3×10^{-15} cm^3 molecule^{-1} s^{-1}.[14] Even if this reaction produced SH (which is $\sim$3.3 kcal mol^{-1} endothermic at 298 K), it could not regenerate SH on the time scale of our experiments. The first-order rate constant for the loss of SH, k^I, was evaluated both in the presence and in the absence of O_2. This rate constant is attributed to the sum of the losses of SH due to self-reaction, reaction with any impurities in the reactor, diffusion out of the reaction zone (defined as the intersection volume between the photolysis and the probe laser beams), and reaction with N_2O

TABLE 1: Experimental Conditions and Results in the Pulsed 193 nm Photolysis Laser-Induced Fluorescence System

conditions label and temp	photolysis fluence (mJ cm^{-2} pulse^{-1})	pressure (Torr) and gas	$[O]_0$ (atom cm^{-3}) from N_2O photolysis	$[N_2O]$ (molecule cm^{-3})	$k' \pm \sigma$ (s^{-1})
PL1,[a] $T = 295$ K	0.02	110 (N_2)	0	0	36 ± 1
			5×10^{11}	2.8×10^{17}	43 ± 1
			4×10^{11}	2.3×10^{17}	37 ± 2
			2×10^{11}	1.0×10^{17}	38 ± 2
			5×10^{11}	2.8×10^{17}	39 ± 2
			1×10^{11}	7.7×10^{16}	35 ± 1
			7×10^{10}	3.9×10^{16}	36 ± 1
			2×10^{10}	1.3×10^{16}	35 ± 1
			0	0	35 ± 2
			5×10^{9}	3.1×10^{15}	36 ± 1
PL2,[b] $T = 294$ K	7	100 (He)	7×10^{13}	1.1×10^{17}	67 ± 13
			5×10^{13}	8.0×10^{16}	61 ± 9
			3×10^{13}	4.3×10^{16}	54 ± 6
			9×10^{12}	1.4×10^{16}	50 ± 8
			0	0	46 ± 4
			0	0	51 ± 5
			9×10^{12}	1.5×10^{16}	49 ± 4
			3×10^{13}	4.4×10^{16}	52 ± 8
			5×10^{13}	8.7×10^{16}	61 ± 15
PL3,[c] $T = 295$ K	0.04	95 (N_2)	0	0	7300 ± 150
			1×10^{10}	3.5×10^{15}	7836 ± 220
			6×10^{11}	1.7×10^{17}	8048 ± 103
			4×10^{11}	1.1×10^{17}	8156 ± 92
			0	0	9255 ± 212
			2×10^{11}	4.3×10^{16}	8330 ± 151
			1×10^{11}	2.8×10^{16}	7773 ± 116
			4×10^{11}	1.2×10^{17}	7826 ± 94
			1×10^{12}	3.7×10^{17}	8108 ± 100
PL4,[d] $T = 295$ K	0.03	100 (N_2)	0	0	53 ± 2
			4×10^{11}	1.6×10^{17}	57 ± 2
			1×10^{11}	5.8×10^{16}	59 ± 2
			2×10^{11}	8.5×10^{16}	53 ± 1
			0	0	51 ± 1
			9×10^{9}	3.4×10^{15}	49 ± 1
PL5,[e] $T = 296$ K	0.5	82 (He)	1×10^{10}	2.7×10^{14}	24 ± 3
	0.5		1×10^{10}	3.0×10^{14}	16 ± 1
	0.5		4×10^{10}	9.0×10^{14}	21 ± 1
	0.5		8×10^{10}	1.8×10^{15}	27 ± 3
	0.5		2×10^{11}	4.0×10^{15}	29 ± 5
	0.5		0	0	20 ± 1
	0.06		0	0	30 ± 1
	0.06		2×10^{10}	3.9×10^{15}	31 ± 2

[a] $[H_2S] = 3.4 \times 10^{14}$ molecules cm^{-3} and $[SH]_0 \approx 5 \times 10^{10}$ molecules cm^{-3} with $[O_2] = 1.2 \times 10^{17}$ molecules cm^{-3}. [b] $[H_2S] = 7 \times 10^{13}$ molecules cm^{-3} and $[SH]_0 \approx 3 \times 10^{12}$ molecules cm^{-3}. [c] $[H_2S] = 3.4 \times 10^{14}$ molecules cm^{-3} and $[SH]_0 \approx 1 \times 10^{10}$ molecules cm^{-3} with $[NO_2] \approx 1 \times 10^{14}$ molecules cm^{-3}. [d] The listed k's are taken from the time constants fit to a biexponential form. $[H_2S] = 8.9 \times 10^{13}$ molecules cm^{-3} and $[SH]_0 \approx 2 \times 10^{10}$ molecules cm^3. [e] For the experiments where the photolysis fluence is 0.5 mJ cm^{-2} pulse^{-1}, the H_2S concentration is 1.4×10^{14} molecules cm^{-3} and where the fluence is 0.06 mJ cm^{-2} pulse^{-1}, the H_2S concentration is 6.3×10^{14} molecules cm^{-3}. This implies that $[SH]_0$ is 4×10^{11} and 2×10^{11} molecules cm^{-3}, respectively.

or other species generated via laser photolysis.

$$SH + SH \rightarrow \text{products} \quad (5)$$

$$SH + \text{impurities} \rightarrow \text{products} \quad (6)$$

$$SH \rightarrow \text{diffusion from reaction zone} \quad (7)$$

$$SH + N_2O \rightarrow \text{products} \quad (1)$$

$$SH + X \rightarrow \text{products} \quad (8)$$

X in reaction 8 is a photoproduct (e.g., $O(^3P)$ and NO) produced in the system whose concentration increases proportionately with that of N_2O. Loss of SH via processes 5−7 is represented as first order in [SH] with an associated first-order rate coefficient denote by k_d. (Reaction 5 is second order in SH; however, over the time scales of the measurements with the low initial SH concentrations that were used, it can be roughly represented as a first-order process.) The overall first-order SH decay rate constant is given by

$$k^I = k_d + k'_1 + k'_X \quad (I)$$

where $k'_1 = k_1[N_2O]$ and k'_X represents the sum of the first-order rate coefficients for the removal of SH with all photoproducts. Note that O_2 does not react rapidly with SH.[3] The concentration of O atoms from the 193 nm photolysis of O_2 was less than 10^9 atoms cm^{-3} and did not contribute significantly to SH loss.

The temporal profiles of SH were measured at various concentrations of N_2O and analyzed to extract k^I. Experimental conditions such as the laser fluence (0.02−7 mJ cm^{-2}) and the SH precursor concentration (1×10^{13} to 4×10^{15} molecules cm^{-3}) were also varied. Table 1 presents the results of these experiments. A plot of the measured pseudo-first-order rate constant for loss of SH vs $[N_2O]$ is shown in Figure 4. To place k'_1 from all the experiments on the same plot, the value of k_d measured in the absence of N_2O (and associated with each set

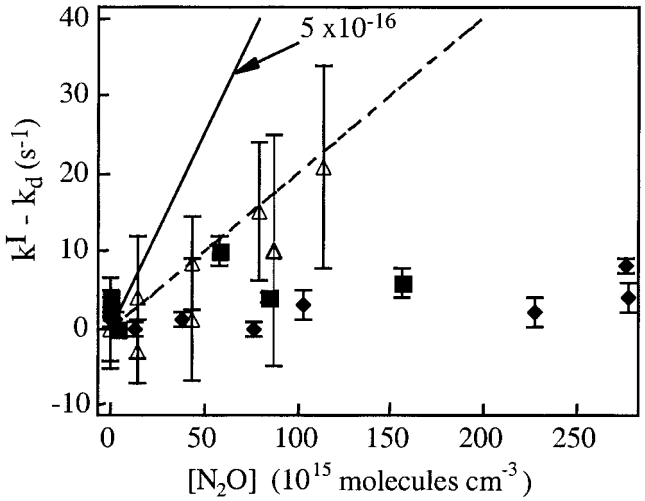

Figure 4. Plot of the first-order rate coefficient for the loss of SH (after subtracting the contribution due to removal in the absence of N_2O) measured in the PP-LIF system as a function of N_2O concentration. The fitted slope plus the 95% confidence interval (dashed line) is 2×10^{-16} cm^3 molecule^{-1} s^{-1}. The solid black line is the upper limit this work (PP-LIF and DF-CIMS) places on k_1 (5×10^{-16} cm^3 molecule^{-1} s^{-1}). The various symbols represent different sections of data found in Table 1. The open triangles are the PL2 data, the squares are the PL4 data, and the diamonds are the PL1 data. The PL3 data are omitted from this figure because the imprecision in that data would make the data presented here difficult to see. The PL5 is omitted as well; it spans a limited concentration range and is clearly affected by secondary reactions (see Discussion).

of measured k_1' values) has been subtracted. The data in Figure 4 are fit to eq II,

$$k^{\mathrm{I}} - k_{\mathrm{d}} = k_1[\mathrm{N_2O}] + k_{\mathrm{X}}' \qquad \text{(II)}$$

using an unweighted linear least-squares method. Note that k_{X}' may vary linearly with [N_2O] and may contribute to the measured slope. The slope of this plot, plus the 95% confidence interval (derived from the precision of the fit), is 2×10^{-16} cm^3 molecule^{-1} s^{-1}. This is the upper limit for k_1 based only on the PP-LIF measurements, excluding the possible systematic influences considered in Discussion.

The temporal profiles of SH measured in He (see Table 1, PL2 subset) using a photolysis fluence of 7 mJ pulse^{-1} cm^{-2} did not obey pseudo first-order kinetics. The pseudo first-order rate constants were determined by fitting the temporal profile after excluding the sharper initial decay and are shown in Table 1 and Figure 4 for the PL2 experiments. In all cases, some N_2O was unavoidably photolyzed to produce O(^{1}D); however, in the PL2 experiments, the fluence was so large that the concentration of initially produced O(^{1}D) was $\sim 10^{13}$ molecules cm^{-3}. The implications of the generation of the high concentration of O(^{1}D) will be discussed later.

Another set of experiments was conducted with a roughly constant amount of NO_2 present in the reaction mixture (PL3). They are not shown because there is a large offset in k' vs [N_2O] for these data (7300 ± 150 s^{-1}), due to the reaction of SH with NO_2. The values of k^{I} for these data show no clear positive influence of N_2O (3.5×10^{15} to 3.7×10^{17} molecules cm^{-3}) on the loss rate constants of SH. These data considered alone yield a rate constant for the title reaction of 8×10^{-16} cm^3 molecule^{-1} s^{-1}; however, these experiments were performed strictly as a crude measurement of k_1 in a system where SH is lost rapidly. Additional implications of these experiments are considered in Discussion.

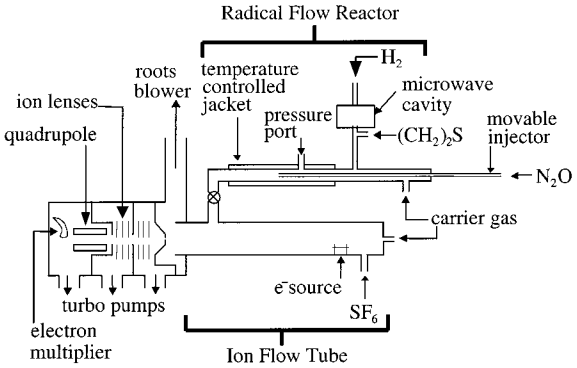

Figure 5. Schematic of the discharge flow CIMS apparatus. SH radicals were generated in a microwave cavity in the sidearm of the flow reactor, and N_2O entered the reactor through a movable injector.

DF-CIMS. A schematic of the discharge flow chemical ionization mass spectrometer (DF-CIMS) instrument used in this study is shown in Figure 5. This instrument has been used previously to measure rate coefficients for various reactions.[15,16] Therefore, only the details associated with the present measurements are discussed.

A 1% mixture of H_2 in UHP He was passed through an active metal trap to remove O_2 and H_2O impurities before flowing through a microwave cavity. The H atoms generated in the microwave discharge reacted with an excess of ethylene sulfide ($(5-20) \times 10^{13}$ molecules cm^{-3}) in a sidearm reactor to produce the SH radical:[17,18]

$$\mathrm{H} + (\mathrm{CH_2})_2\mathrm{S} \rightarrow \mathrm{SH} + \mathrm{C_2H_4} \qquad (9)$$

Reaction 9 ($k_9 = 1.2 \times 10^{-12}$ cm^3 molecule^{-1} s^{-1}) was allowed to go to completion (i.e., typically greater than three lifetimes in [H]) before SH came into contact with N_2O. N_2O was added through a 9.5 mm movable Teflon injector downstream of the SH generation region. Thus, SH generation by reaction 9 was insignificant after the mixture encountered N_2O. A 2.22 cm i.d. Teflon sleeve lined the inside of the flow reactor to minimize radical loss on the reactor walls. Flow rates of N_2O (0.001−1.1 STP cm^3 s^{-1}; STP = 1 atm, 273 K) were calculated from the time rate of change of pressure in a calibrated volume. Concentrations of N_2O in the flow reactor were 1.5×10^{13} to 2.2×10^{16} molecules cm^{-3}. Up to 10 STP cm^3 s^{-1} of UHP (>99.9995%) He was passed through a liquid nitrogen trap and added to the flow reactor to serve as a carrier gas. The pressure in the middle of the 50 cm reaction zone, 1.2−1.9 Torr, was measured using a calibrated capacitance manometer.

In the ion flow tube, SH radicals exiting the radical flow reactor were converted to SH^- via charge transfer with the SF_6^- reagent ion:

$$\mathrm{SF_6^-} + \mathrm{SH} \rightarrow \mathrm{SF_6} + \mathrm{SH^-} \qquad (10)$$

The SF_6^- ion was generated at the upstream end of the ion flow tube by passing a small flow of SF_6 over an electron-emitting filament. Up to 120 STP cm^3 s^{-1} of He was added to the 7.30 cm i.d. stainless steel ion flow tube, where the total pressure was approximately 0.6 Torr. SH^- was mass-selected with a quadrupole mass filter and detected by an electron multiplier. SH concentrations of less than 1×10^{10} molecules cm^{-3} in the flow reactor were estimated for all the kinetics experiments on the basis of the measured SH^- signal levels and an assumed rate coefficient for the reaction of SH with SF_6^- of 2×10^{-9}

TABLE 2: Experimental Conditions and Results in the Discharge Flow Chemical Ionization Mass Spectrometry System

		$[N_2O]$ (molecule cm^{-3})	$k' \pm \sigma$ (s^{-1})
	DF1		
pressure	1.28−1.77 Torr	0	-4.5 ± 0.6
temperature	295 K	0	-4.6 ± 0.4
main flow velocity	1169−1465 cm s^{-1}	0	-17.3 ± 0.5
		3.27×10^{15}	-15.3 ± 0.8
		9.81×10^{15}	-4.3 ± 0.9
		1.71×10^{16}	-7.7 ± 0.6
		2.19×10^{16}	-21.0 ± 0.5
	DF2		
pressure	1.30−1.57 Torr	0	-14.7 ± 1.0
temperature	295 K	0	-13.9 ± 1.0
main flow velocity	1219−1357 cm s^{-1}	6.02×10^{15}	-20.9 ± 1.1
		8.93×10^{15}	-16.4 ± 1.1
		1.65×10^{16}	-20.0 ± 1.2
	DF3		
pressure	1.31−1.44 Torr	0	-10.5 ± 0.2
temperature	295 K	0	-12.3 ± 0.5
main flow velocity	1175−1301 cm s^{-1}	0	-11.9 ± 0.3
		1.57×10^{13}	-12.0 ± 0.4
		1.57×10^{13}	-12.5 ± 0.3
		6.69×10^{14}	-11.5 ± 0.4
		1.15×10^{15}	-11.5 ± 0.6
		5.76×10^{15}	-12.0 ± 0.3
	DF4		
pressure	1.32−1.56 Torr	0	-20.4 ± 0.6
temperature	295 K	1.85×10^{13}	-17.0 ± 0.6
main flow velocity	1369−1439 cm s^{-1}	1.01×10^{14}	-18.4 ± 0.7
		4.22×10^{14}	-17.9 ± 0.7
		1.47×10^{15}	-19.2 ± 1.1
		5.52×10^{15}	-19.0 ± 0.9
		$[N_2]$ molecule cm^{-3}	$k' \pm \sigma$ (s^{-1})
	DF5		
pressure	1.30−1.49 Torr	0	-17.7 ± 1.0
temperature	295 K	1.93×10^{13}	-14.9 ± 0.7
main flow velocity	1377−1480 cm s^{-1}	9.80×10^{13}	-15.9 ± 0.7
		1.23×10^{14}	-12.5 ± 0.5
		4.08×10^{14}	-12.8 ± 0.7
		4.98×10^{15}	-20.0 ± 0.8
		$[NO_2]$ molecule cm^{-3}	$k' \pm \sigma$ (s^{-1})
	DF6		
pressure	1.27−1.36 Torr	0	-8.25 ± 0.3
temperature	343 K	9.63×10^{10}	-5.68 ± 0.5
main flow velocity	1552−1650 cm s^{-1}	2.64×10^{11}	19.65 ± 0.9
		3.72×10^{11}	16.68 ± 0.9
		8.38×10^{11}	59.69 ± 1.1
		1.20×10^{12}	69.24 ± 2.2
		1.61×10^{12}	105.78 ± 3.5

cm^3 molecule^{-1} s^{-1}. Typically, exothermic electron-transfer reactions such as reaction 10 proceed at the Langevin collisional rate.

Reaction 1 was studied under pseudo-first-order conditions in SH by monitoring the SH^- signal as a function of injector position. The SH^- signal level is proportional to the concentration of SH at the end of the ion flow tube. The variation of the SH^- signal with reaction distance was fitted to expression III using a weighted least-squares method,

$$S_{SH^-} = A \exp(-k'd/v) + C \qquad \text{(III)}$$

In this expression,

$$k' = k_1[N_2O] + k_{loss} \qquad \text{(IV)}$$

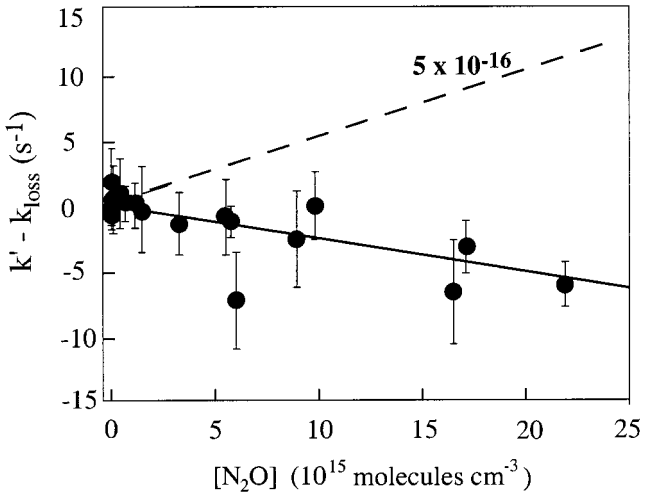

Figure 6. Plot of $k' - k_{loss}$, measured using the discharge flow CIMS apparatus, as a function of $[N_2O]$ in the reactor. The solid line is a weighted linear fit to the data yielding $(-2.5 \pm 1.5) \times 10^{-16}$ cm^3 molecule^{-1} s^{-1}. Error bars represent the combined 95% confidence intervals for the fits of k' and k_{loss}. The reported limit of $k_1 < 5 \times 10^{-16}$ cm^3 molecule^{-1} s^{-1} is plotted as a dashed line.

where k_{loss} is the first-order rate constant for removal of SH in the absence of N_2O, d is the relative reaction distance, v is the average linear gas flow velocity in the flow reactor downstream of the injector, and C represents an experimental background signal at this mass. The DF-CIMS results are presented in Table 2. Loss of SH radicals on the outer wall of the injector led to a rise in SH^- signal as the injector was retracted so that the measured k' values were negative. This is generally observed in flow tube studies where the monitored radical is in the main body of the flow tube and the excess reactant is introduced through a movable injector, as in the present work. Decay constants obtained in the absence of N_2O (i.e., k_{loss}) were subtracted from those measured in the presence of N_2O (k'). The rate constant difference ($k' - k_{loss}$) ranged from -7.4 to 1.7 s^{-1} and typically encompassed zero within 2σ of the measured value of k'. Figure 6 shows a plot of ($k' - k_{loss}$) measured at various concentrations of N_2O. It is clear that there is no discernible change in ($k' - k_{loss}$) upon addition of N_2O. A weighted linear fit of these data yields a slope of $(-2.5 \pm 1.5) \times 10^{-16}$ cm^3 molecule^{-1} s^{-1} at room temperature. Error bars are determined by combining the 95% confidence intervals of the fits to eq III for k' and k_{loss}.

Obviously, a rate coefficient cannot be negative. The negative slope may be due to complex SH diffusion behavior in the flow reactor. With only the He carrier gas present, SH radicals that are lost on the flow reactor walls are replaced via fast diffusion. This first-order wall loss of radicals is independent of injector position and is not represented in the observed decays. However, when a significant amount of N_2O is added through the injector, the effective diffusion constant for SH in the flow reactor decreases and radical loss at the reactor wall is inhibited. Retracting the injector exposes more of the SH stream to N_2O, resulting in a greater increase of SH signal than without N_2O present. Thus, high concentrations of N_2O may serve to make k' more negative, as seen in Figure 6. In the DF-CIMS experiments, N_2O was as much as 40% of the flow reactor content. A simulation of the conditions in the flow reactor suggests that up to 30% of the observed ($k' - k_{loss}$) can be accounted for by depressed radical wall loss.

To test that the negative k_1 value was due to SH diffusion effects and not to secondary chemistry in the flow reactor, a

series of experiments was performed with N_2 (an inert species) in place of N_2O. The variation of k' with $[N_2]$ is similar to that seen with N_2O. Since N_2 does not react with SH, this experiment lends support to the low measured value of k_1. The line representing a k_1 value of 5×10^{-16} cm^3 molecule^{-1} s^{-1} is also shown in the figure. Clearly, the measured values are consistent with an upper limit of 5×10^{-16} cm^3 molecule^{-1} s^{-1}.

Discussion

As shown above, we did not observe a reaction between SH and N_2O in the pulsed photolysis system. An upper limit for k_1 is 2×10^{-16} cm^3 molecule^{-1} s^{-1}, based on the pulsed photolysis experiments. This result is consistent with the upper limit of 5×10^{-16} cm^3 molecule^{-1} s^{-1} derived from the flow tube studies. Similar results from two distinctly different experimental methods that do not have the same sources of systematic errors lend confidence to our conclusion that reaction 1 is slow. It is conceivable, though, that reaction 1 occurs rapidly, but in these experiments, SH does not *appear* to react with N_2O. Therefore, we examined possible mechanisms that would mask the occurrence of reaction 1 in our systems. The quantification of these considerations leads to our final result, $k_1 < 5 \times 10^{-16}$ cm^3 molecule^{-1} s^{-1}. We also explore below a possible reason for the large value of k_1 reported by Ravichandran et al.[4]

Secondary Chemistry in the PP-LIF System. The SH radical may be regenerated by secondary reactions whose rates in our systems scale with N_2O concentration and thus obscure reaction 1. This possibility is explored below for the pulsed photolysis system. The reactions that can occur following photolysis of a mixture of H_2S and N_2O at 193 nm are

$$H_2S \xrightarrow{h\nu/193\ \text{nm}} H + SH \quad (2)$$

$$HS + N_2O \rightarrow HSO + N_2 \quad (1)$$

$$H + H_2S \rightarrow HS + H_2 \quad (3)$$

$$N_2O \xrightarrow{h\nu/193\ \text{nm}} N_2 + O(^1D) \quad (11)$$

$$O(^1D) + N_2 \rightarrow O(^3P) + N_2 \quad (12)$$

$$O(^1D) + N_2O \rightarrow O_2 + N_2 \quad (13a)$$

$$O(^1D) + N_2O \rightarrow 2NO \quad (13b)$$

$$O(^3P) + H_2S \rightarrow OH + SH \quad (14)$$

$$O(^3P) + HS \rightarrow OH + S \quad (15a)$$

$$O(^3P) + HS \rightarrow SO + H \quad (15b)$$

$$HSO + N_2O \rightarrow N_2 + O_2 + SH \quad (16)$$

Influence of the Reaction of $H + H_2S$. If SH is regenerated by reaction 3 on the time scale of reaction 1, we may not observe a loss of SH in our systems. Analyses of the biexponential temporal profiles (see Figure 3) yielded time constants for the rise that agreed with the rate coefficient for reaction 3. Furthermore, as expected, the rise time for SH increased with H_2S concentration. The rise time of SH should scale only with $[H_2S]$ because H atoms do not react rapidly with N_2O or O atoms. The rate coefficient for the loss of SH derived from the biexponential fits in the absence of N_2O was the same as those in the presence of N_2O. In addition, when O_2 was added in sufficient quantities to scavenge H atoms, the decay rate constant for SH did not change within the precision of the measurements; however, the initial rise in SH due to reaction 3 was essentially eliminated, as one anticipates (see Figure 3). The lifetime of H in 3.5 Torr of O_2 and 1 mTorr of H_2S with a total pressure of 100 Torr of N_2 is 44 μs, on the basis of the known rate coefficients[3] for reactions 3 and 4. This time constant is much shorter than the lifetime of SH observed in our experiments. Also, in one series of experiments, NO_2 was added to scavenge H atoms and the obtained value of k_1 was essentially the same. On the basis of these arguments, we rule out the possibility of SH regeneration via reaction 3 as a significant source of error in measuring k_1.

Influence of the Reaction of $O + H_2S$. The concentration of $O(^1D)$ produced through the unavoidable photolysis of N_2O at 193 nm scales with N_2O concentration. In the PP-LIF reactor, $O(^1D)$ is collisionally quenched to $O(^3P)$ by N_2 within 0.2 μs (calculated five lifetimes for 30 Torr, the lowest pressure that was employed). A fraction of $O(^1D)$ also reacts with N_2O to make N_2, O_2, and NO (reaction 13). The presence of O atoms can alter the temporal behavior of SH in two ways: (a) it can generate SH via reaction 14 and (b) it can deplete SH via reaction 15 and, to a lesser extent, via addition to NO. At a fixed concentration of N_2O, the laser fluence was varied by a factor of 25 to proportionately change the initial O atom concentration ($[O]_{max} < 1 \times 10^{12}$ atom cm^{-3}) and, hence, its contribution to SH loss. The contribution of O atoms was identified to be negligible because the measured value of k_1, within the precision of the measurements, did not change (see PL1 and PL5 in Table 1). The regeneration of SH via reaction 14, even though it results in the production of two SH radicals (because the OH product in this reaction will rapidly react with H_2S to give a second SH), is relatively slow ($k_{14}(298K) \approx 2 \times 10^{-14}$ cm^3 molecule^{-1} s^{-1}) and should be negligible; i.e., the first-order rate constant for regeneration of SH is less than 2 s^{-1}. Changing the concentration of H_2S did not change the measured value of k_1 and again confirms the expected negligible contribution of reaction 14 (see Table 1).

With the exception of the data taken at high fluence and/or He bath gas, photolysis of N_2O generated less than 1×10^{12} molecules cm^{-3} of $O(^3P)$. The rate constant for the reaction of $O(^3P)$ with SH is approximately gas kinetic[19] and can lead to an initial rapid loss of SH with a first-order rate constant of up to 100 s^{-1}. We scavenged $O(^3P)$ by adding O_2 and reduced the SH loss via reaction with O atom by a factor of at least 3; the measured first-order rate coefficient for SH loss did not change. Therefore, we conclude that the O atom reactions did not contribute to the measured small value of k_1. If HO_2 reacts with the SH radical as quickly as it does with the OH radical[3] (1.1×10^{-11} cm^3 molecule^{-1} s^{-1}), the rate constant for the initial loss of SH radical could be enhanced by as much as 10 s^{-1}. This enhancement was estimated from the calculated concentration of HO_2 generated in the experiments when O_2 was added to scavenge H atoms. The increase is a negligible change to the decay rate constants.

It should be noted that none of the secondary reactions mentioned above (reactions 3, 14, and 15) are important in the DF-CIMS experiment, which yielded the same results as the pulsed photolysis measurements.

SH Radical Detection in the DF-CIMS System. To validate the SH detection methodology in the flow tube experiments, the rate coefficient for the reaction of SH with NO_2,

$$SH + NO_2 \rightarrow HSO + NO \quad (17)$$

was also measured in a procedure analogous to that used to measure k_1. At 343 K and 1.3 Torr, the rate coefficient for reaction 17 was measured to be $(7.0 \pm 0.9) \times 10^{-11}$ cm^3 molecule^{-1} s^{-1}, in reasonable agreement with the accepted value[17] of $(5.9 \pm 1.0) \times 10^{-11}$ cm^3 molecule^{-1} s^{-1}. This experiment confirms that the SH^- signal seen in our system is due primarily to the SH radical inside the flow reactor.

Possibility of SH Regeneration from Reaction of HSO(A^2A') with N_2O. It is possible that the reaction of SH with N_2O produces HSO(A^2A').

$$SH + N_2O \rightarrow HSO(A^2A') + N_2 \qquad \Delta_r H°(298K) = -7.8 \text{ kcal mol}^{-1} \quad (18)$$

The heat of formation of HSO(A^2A') was calculated from the known energy separation, ~47 kcal mol^{-1}, between HSO(X) and HSO(A) states. Further, the reaction of HSO(A^2A') with N_2O to give SH (reaction 19) is exothermic:

$$HSO(A^2A') + N_2O \rightarrow SH + N_2 + O_2 \qquad \Delta_r H°(298K) = -31 \text{ kcal mol}^{-1} \quad (19)$$

The reaction of HSO(X) with N_2O is endothermic by ~16 kcal mol^{-1} and is not expected to occur (see below). If reactions 18 and 19 both occur, they could mask reaction 1. The quenching rate coefficients[20] of HSO(A^2A') by He and N_2 are $\sim 2.5 \times 10^{-12}$ and $\sim 5 \times 10^{-12}$ cm^3 molecule^{-1} s^{-1}, respectively. The fraction of HSO(A^2A') that could react with N_2O is ~0.6, in 100 Torr of N_2 and 10 Torr of N_2O, if we assume k_{19} to be 1×10^{-10} cm^3 molecule^{-1} s^{-1}. In our experiments, the measured rate constant did not change with N_2O concentration. Even with 10 Torr of N_2O, the fraction of HSO(A^2A') that is quenched is ~0.4, and therefore, this scenario could mask the measurement of k_1 by a factor of at most 2.5, not orders of magnitude from the real value. At lower concentrations of N_2O, this quenching fraction would be smaller and regeneration, if it occurs at all, would be lower. Therefore, we conclude that the possible reaction of HSO(A^2A') with N_2O is not responsible for the low measured value of k_1 compared to that previously reported. This conclusion is supported by the upper limit determined using the flow tube where N_2O concentrations were in the milliTorr range.

In one series of experiments (PL3), $\sim 1 \times 10^{14}$ molecules cm^{-3} of NO_2 was added. In this case, HSO is produced by reaction 17. Reaction 17 is exothermic by ~21 kcal mol^{-1}. If HSO(X), the product of reaction 17, contained all the excess energy of the reaction, it could react with N_2O to produce SH. In such a case, the measured SH decays would have been reduced upon addition of N_2O. Such a decrease was not seen (see PL3). This lack of regeneration is not proof that energetic HSO does not react with N_2O but is consistent with the absence of such a reaction.

Possible Reason for the Discrepancy between Our Values and Those of the Previous Report. We quote an upper limit for k_1 of less than 5×10^{-16} cm^3 molecule^{-1} s^{-1} at 298 K. This upper limit is 4 orders of magnitude smaller than the value reported by Ravichandran et al.[4] We offer the following mechanism/scenario as a possible explanation for the observations of Ravichandran et al. We emphasize that we do not have sufficient information or familiarity with their apparatus and experiments to properly interpret their observations.

Though they mention that LIF may be used to detect HSO and SH, Ravichandran et al. did not present such data in their paper. Therefore, we will discuss only their chemiluminescence data. The high value of the rate coefficient reported by Ravichandran et al. may be due to an incorrect interpretation of their observations. These authors measured the chemiluminescence from HSO(A^2A') upon photolysis of mixtures of H_2S and N_2O at total pressures of 0.5−4 Torr. Ravichandran et al. appear to have relied on the temporal profile of the HSO* chemiluminescence signal to extract a value of k_1. The authors ruled out the possibility that reactions of SH with O(^{1}D) or O(^{3}P) are responsible for the HSO signal. It appears from their published paper that they did not consider the possibility that the reaction of O(^{1}D) with H_2S could yield HSO(A^2A'):

$$O(^1D) + H_2S \rightarrow HSO(A^2A') + H \qquad \Delta_r H°(298) = -2 \text{ kcal mol}^{-1} \quad (20)$$

This reaction may occur because O(^{1}D) has a propensity to insert into stable molecules and the excited HSOH may eliminate an H atom. Note that only a very small fraction of the O(^{1}D)−H_2S encounter needs to produce chemiluminescence to obtain a strong signal.

The apparent rate constants for the rise and decay of the HSO chemiluminescence signals in Figure 3 of the Ravichandran et al. paper are on the order of 10 and 1 μs^{-1}, respectively. In their Figure 4, they identified the rise as due to production of HSO* (their panel a) and decay as to loss of HSO* (their panel b). Figure 4a (labeled as production of HSO) has a slope that would correspond to a bimolecular rate constant of 1.3×10^{-11} cm^3 molecule^{-1} s^{-1}, identified by them as the rate coefficient for the reaction of SH with N_2O. Their Figure 4b (labeled as loss of HSO) has a slope corresponding to a bimolecular rate constant of 1.5×10^{-10} cm^3 molecule^{-1} s^{-1}, which the authors associated with the rate coefficient for the removal of HSO*. Their assignment may be in contradiction with their Figure 3. Without external calibration of the signal and/or a priori knowledge of the rates of processes, it is not possible to determine which part of the biexponential profile corresponds to the formation of HSO* and which corresponds to its quenching.[21] Their reported value of $k_1 = 1.3 \times 10^{-11}$ cm^3 molecule^{-1} s^{-1} may be the rate coefficient for the quenching of HSO(A^2A') by N_2O (reaction 21), while the faster rate coefficient may be for the reaction of O(^{1}D) with N_2O in the following sequence of processes in their system:

$$N_2O \xrightarrow{h\nu/193 \text{ nm}} N_2 + O(^1D) \quad (11)$$

$$O(^1D) + N_2O \rightarrow O_2 + N_2 \quad (13a)$$

$$O(^1D) + N_2O \rightarrow 2NO \quad (13b)$$

$$O(^1D) + H_2S \rightarrow HSO(A^2A') + H \quad (20)$$

$$HSO(A^2A') + N_2O \rightarrow HSO(X) + N_2O \quad (21)$$

In the above scheme, the rise time would increase with N_2O because both reactions 13 and 20 control that time constant. Of course, in their experiments the signal level (due to HSO(A^2A')) may not change with N_2O concentration because N_2O is both the source of O(^{1}D) and the reactant for O(^{1}D). Ravichandran et al. also reported that they detected vibrationally excited HSO(A), i.e., HSO(A^2A', $v' \leq 5$). If the thermochemistry of

HSO(X) is correct and O(^{1}D) is thermalized in their system, then reaction 20 cannot be the source of their observed HSO(A^2A', $v' \leq 5$). However, it is worth noting that thermalizing the translational energy of O(^{1}D) in a system where it is reacting almost on every collision with a reactant is difficult if only a small amount of a thermalizing agent, such as an unreactive bath gas, is added.

The same authors also report that vibrational excitation of N_2O to the (1, 0, 0) vibrational state raises their measured rate constant by a factor of 2.2. It is possible that the vibrational excitation of N_2O increases the absorption of 193 nm and yields more O(^{1}D). However, the time constant for the decay of HSO(A^2A') signal should not change, unless vibrationally excited N_2O quenched HSO(A^2A') more efficiently. If N_2O(1, 0, 0) was produced after HS was produced and the same enhancement was observed, our explanation of what could have caused the faster appearance of HSO(A) would be wrong. The main reason we proposed a plausible scheme is to show that there are reasons to suspect the results of Ravichandran et al. and not to unequivocally identify where their measurements or interpretations were in error. An incorrect explanation on our part for the large value of the rate constant reported by Ravichandran et al. does not affect our conclusion that SH does not react rapidly with N_2O.

Atmospheric Implications. Our upper limit of k_1 at 298 K is less than 5×10^{-16} cm^3 molecule^{-1} s^{-1}. This value should be also applicable under most atmospheric temperatures. Our small rate coefficient suggests that reaction 1 does not impact ($<4 \times 10^{-4}$%) the loss rate of SH in the troposphere. Further, this reaction should not significantly alter the calculated lifetime of N_2O in the atmosphere. Even if we take a very high globally averaged tropospheric concentration of SH of 1×10^3 cm^{-3}, the lifetime of N_2O with respect to this reaction would be ~60 000 years, based on our measured upper limit for k_1. Such a slow chemical sink in the troposphere would reduce the atmospheric lifetime of N_2O by at most 0.2%. Therefore, we conclude that the reaction of SH with N_2O is not significant to the chemistry of earth's atmosphere.

References and Notes

(1) Berresheim, H.; Wine, P. H.; Davis, D. D. Sulfur in the atmosphere. In *Composition, Chemistry and Climate of the Atmosphere*; Singh, H. B., Ed.; Van Nostrand Reinhold: New York, 1995; pp 251−307.

(2) Tyndall, G. S.; Ravishankara, A. R. *Int. J. Chem. Kinet.* **1991**, *23*, 483−527.

(3) DeMore, W. B.; Sander, S. P.; Golden, D. M.; Hampson, R. F.; Kurylo, M. J.; Howard, C. J.; Ravishankara, A. R.; Kolb, C. E.; Molina, M. J. *Chemical Kinetics and Photochemical Data for Use in Stratospheric Modeling*; Evaluation 12, JPL Publication 97-4; Jet Propulsion Laboratory: Pasadena, CA, 1997.

(4) Ravichandran, K.; Williams, R.; Fletcher, T. R. *Chem. Phys. Lett.* **1994**, *217*, 375−379.

(5) World Meteorological Organization, Report 44, *Scientific Assessment of Ozone Depletion*: 1998; Geneva, Switzerland, 1999, p 1.3.

(6) Assuming a globally averaged H_2S emission rate of 1 Tg of S per year, a lifetime of SH of 0.3 s, and steady state in H_2S and SH concentrations, we calculate the $[SH]_{av}$ to be 115 molecules cm^{-3} at ground level. The concentration of SH will approximately fall off linearly with number density as the altitude increases.

(7) Biermann, H. W.; Zetzsch, C.; Stuhl, F. *Ber. Bunsen-Ges. Phys. Chem.* **1976**, *80*, 909.

(8) Vaghjiani, G. L.; Ravishankara, A. R. *J. Phys. Chem.* **1989**, *93*, 1948−1959.

(9) Turnipseed, A. A.; Barone, S. B.; Ravishankara, A. R. *J. Phys. Chem.* **1994**, *97*, 5926−5934.

(10) Weiner, B. R.; Levene, H. B.; Valentini, J. J.; Baronavski, A. P. *J. Chem. Phys.* **1989**, *90*, 1403.

(11) Kakimoto, M.; Saito, S.; Hirota, E. *J. Mol. Spectrosc.* **1980**, *80*, 334−350.

(12) Kurylo, M. J.; Peterson, N. C.; Brown, W. *J. Chem. Phys.* **1971**, *54*, 943.

(13) Bradley, J. N.; Trueman, S. P.; Whytock, D. A.; Zaleski, T. A. *J. Chem. Soc., Faraday Trans. I* **1973**, *69*, 416.

(14) Mellouki, A.; Ravishankara, A. R. *Int. J. Chem. Kinet.* **1994**, *26*, 355−365.

(15) Lovejoy, E. R.; Hanson, D. R.; Huey, L. G. *J. Phys. Chem.* **1996**, *100*, 19911.

(16) Froyd, K. D.; Lovejoy, E. R. *Int. J. Chem. Kinet.* **1999**, *31*, 221.

(17) Wang, N. S.; Lovejoy, E. R.; Howard, C. J. *J. Phys. Chem.* **1987**, *91*, 5743−5749.

(18) Lee, J. H.; Stief, L. J.; Timmons, R. B. *J. Phys. Chem.* **1977**, *67*, 1705−1709.

(19) Cupitt, L. T.; Glass, G. P. *Int. J. Chem. Kinet.* **1975**, *1*, 39−50.

(20) Hung, W.-C.; Lee, Y.-P. *J. Chin. Chem. Soc.* **1993**, *40*, 407−412.

(21) Haugen, H. K.; Pence, W. H.; Leone, S. R. *J. Chem. Phys.* **1984**, *80*, 1839−1852.